

Parity violating gravitational waves at the end of inflation

Mar Bastero-Gil^{1,*} and António Torres Manso^{1,†}

¹*Departamento de Física Teórica y del Cosmos, Universidad de Granada, Granada-18071, Spain*

Inflaton-vector interactions of the type $\phi F\tilde{F}$ have provided interesting phenomenology to tackle some of current problems in cosmology, namely the vectors could constitute the dark matter component. It could also lead to possible signatures imprinted in a gravitational wave spectrum. Through this coupling, a rolling inflaton induces an exponential production of the transverse polarizations of the vector field, having a maximum at the end of inflation when the inflaton field velocity is at its maximum. These gauge particles, already parity asymmetric, will source the tensor components of the metric perturbations, leading to the production of parity violating gravitational waves. In this work we examine the vector particle production with an attempt to mimic its backreaction effects on the inflation evolution in the weak coupling regime. Furthermore, we fully integrate the gauge particle amplitudes spectrum during this production epoch, studying the behavior until the end of reheating. Finally, we calculate the gravitational wave spectrum solely relying on the vector mode WKB expansion in its regime of validity.

I. INTRODUCTION

Cosmological inflation, an early phase of accelerated expansion, is currently the preferred solution to address the flatness and horizon problem in Standard Cosmology [1–3]. Typically a scalar field, the inflaton ϕ , during a slow-roll phase drives such an expansion, and through its quantum vacuum fluctuations gives a natural mechanism to generate the observed anisotropies in the Cosmic Microwave Background (CMB). The question on how to move into the better known Standard Cosmology has to be addressed, including the period known as reheating, the transition into a radiation dominated universe, where production of light nuclei at Big Bang Nucleosynthesis (BBN) takes place [4, 5]. To do so one has to couple the inflaton with other particles species [6].

Inspired by "axion-like" inflation models [7], where a shift symmetry protects the flatness of the inflaton potential, couplings with $U(1)$ vector particles $\alpha\phi F\tilde{F}/f$ are often considered, where α is the coupling constant and f an energy scale. As ϕ rolls down in the slow-roll evolution it will source a tachyonic amplification of the vector modes from their vacuum fluctuations into a classical state. As the interaction parameter will depend linearly on the inflaton velocity, the largest amplification is expected at the end of inflation, as the system escapes the slow-roll evolution¹. Due to the parity violating nature of the interaction only one of the vector transverse degrees of freedom is amplified [11]. This abrupt production of gauge fields may source a sizable production of gravitational waves (GW) [12–15], also parity asymmetric, within a range of frequencies that will depend on the stage of inflation. This could mean an observational signal in the CMB or at interferometer scales.

Phenomenology with these models is extremely broad. For example the production of non-Gaussianities in the primordial comoving curvature perturbations has been studied in [16–18], and provides the strongest bound on the interaction parameters at CMB scales. The inflaton-vector dynamics has also been used to study the production of primordial magnetic fields [11, 19, 20], as a dissipation mechanism allowing inflation with steeper potentials [21] or as an ignition for warm inflation in the case of Yang-Mills gauge interactions [22, 23]. Other studies focus on the generation of different dark sectors, like primordial black hole production [14, 18] but also particle dark sectors [24–31]. Within the later, we may have the vectors as a dark matter candidate, compatible with the observed dark matter relic abundance for masses $\mu\text{eV} \lesssim m \lesssim 10 \text{ TeV}$ [32, 33], or due to the extremely efficient pair production via Schwinger effect when including a fermion-vector coupling [34, 35]. The parity asymmetry within the system has also been exploited to explain the baryon asymmetry in the Universe [36–41].

In this work we will examine the gravitational wave spectrum sourced by the inflaton-vector coupling not only during inflation, but until the onset of a radiation dominated era. End of inflation (accelerated expansion) is set by the condition $\epsilon_H = -\dot{H}/H^2 = 1$, H being the Hubble expansion rate and \dot{H} its time derivative, whereas in a radiation dominated universe one has $\epsilon_H = 2$. In this extra period from $\epsilon_H = 1$ to $\epsilon_H = 2$, one still finds amplitude

*Electronic address: mbg@ugr.es

†Electronic address: atmanso@correo.ugr.es

¹ In regimes with large interaction parameters and considering the backreaction of vector production on inflaton evolution, there are non-linear effects which affects the dynamics and the analysis is not as straightforward, see [8–10].

enhancement in the larger momentum modes that are still sub-horizon at the end of inflation. Indeed, vector particle production can easily take place during preheating [27, 42], i.e., the first stages of the reheating period [43, 44], but typically for coupling values $\alpha m_P/f$ larger than those required to avoid backreaction (BR) effects during inflation. We will therefore stay within the linear, non-backreaction (NBR) regime, for which preheating effects can be ignored. Nevertheless, our main point is that even in this regime where we may expect to be able to treat the transition to radiation perturbatively, particle production continues up to $\epsilon_H = 2$ invalidating the linear analyses. Taking into account this regime, we aim to derive an upper bound on $\alpha m_P/f$ for which non-linear effects may be ignored.

We will take a semi-analytical approach to describe the gauge mode amplitudes that result from the tachyonic amplification sourced by ϕ . It will consist on composing the analytical solution valid to describe the vector amplitudes during the amplification until horizon crossing and the solution obtained numerically at the beginning of radiation domination, when the modes cease to grow. In our analysis we will see that in order to avoid backreaction effects due to vector production at the latter stages of inflation, one must take an interaction parameter $\xi = (\alpha/f)(\dot{\phi}/H)/2$ at 60 e-folds before the end of inflation smaller than what is constrained by non-Gaussianities. We will try a simple scheme, based on energy conservation of the vector modes, to mimic the backreaction effects on the inflaton motion without doing the individual numerical integration for every vector. This will allow us to study systems with $\xi \lesssim 0.85$ at 60 e-folds ($\alpha m_P/f \lesssim 9.78$) with an accurate description. We will find a spectrum of gravitational waves with a peak at very large frequencies, $10^7 \text{ Hz} \lesssim f \lesssim 10^9 \text{ Hz}$, typical of production mechanism at the end of inflation and (p)reheating.

There has been an effort to study the full non-linear regime with different methodologies. Through what is called the gradient expansion formalism, a truncated system of bilinear functions of the electric and magnetic fields in position space, one mimics the backreaction effects and can source the dissipation on the inflaton dynamics. In [9, 45] these integrations were performed until the end of inflation at $\epsilon_H = 1$, thus they do not account for the effects during (p)reheating until $\epsilon_H = 2$. Nevertheless, interesting dynamics results from the backreaction estimation, namely on the oscillating effect on the interaction parameter ξ at the end of inflation and the double peak structure at the spectral energy density of the vector modes. In the work [8] the non-linear evolution of ξ was also obtained, and recently confirmed in [10] after the first lattice computations on gauge particle production in axion inflation.

This paper is organized as follows. In section II we set the model and study the vector production to discuss the validity of the non-backreaction description. We provide a first order attempt to manage the backreaction effects in section III. Finally we calculate the gravitational wave spectrum in section IV, to then conclude and discuss followup work in section V. Technical details about the parametrization used for the vector power spectrum and the calculation of the induced GW spectrum are given respectively in Appendix A and B.

II. VECTOR PARTICLE PRODUCTION

Consider a system described by the action

$$\mathcal{S} = - \int d^4x \sqrt{-g} \left[\frac{1}{2} \partial_\mu \phi \partial^\mu \phi + V(\phi) + \frac{1}{4} F_{\mu\nu} F^{\mu\nu} + \frac{1}{2} m^2 A_\mu A^\mu + \frac{\alpha}{4f} \phi F_{\mu\nu} \tilde{F}^{\mu\nu} \right] \quad (1)$$

where the potential $V(\phi)$ drives the slow-roll evolution, α/f quantifies the inflaton-vector coupling, $F_{\mu\nu}$ is the field strength and $\tilde{F}^{\mu\nu}$ its dual, $\tilde{F}^{\mu\nu} = \epsilon^{\mu\nu\alpha\beta} F_{\alpha\beta} / (2\sqrt{-g})$. We use the Friedmann-Robertson-Walker metric with $ds^2 = -dt^2 + a^2(t)dx^2$ and the convention $\epsilon^{0123} = 1/\sqrt{-g}$. The vector mass can be of a Stueckelberg type or be produced through a symmetry breaking phase transition. It will be considered to be smaller than the Hubble scale at the end of inflation, making it negligible during the tachyonic production.

In our analysis we will consider a quartic inflaton potential, $V(\phi) = \lambda\phi^4/4$. Even though in the simpler implementations it has been ruled out by Planck data [46], constructions with non-minimal kinetic terms or the so called α -attractor models [47] still allow for effective quartic potentials. Furthermore, as the main vector production happens at the end of inflation, this effective description becomes extremely reliable.

In order to study the production of gauge particles induced by the rolling inflaton, we promote the classical field $A(t, x)$ to an operator $\hat{A}(t, x)$, to then be expanded in terms of creation and annihilation operators and the mode functions in an helicity basis

$$\hat{A}_i(t, \mathbf{x}) = \int \frac{d^3\mathbf{k}}{(2\pi)^3} e^{i\mathbf{k}\cdot\mathbf{x}} \hat{A}_i(t, \mathbf{k}) = \sum_{\lambda=\pm, L} \int \frac{d^3\mathbf{k}}{(2\pi)^3} [\epsilon_\lambda^i(\mathbf{k}) A_\lambda(t, \mathbf{k}) \hat{a}_\lambda^{\mathbf{k}} e^{i\mathbf{k}\cdot\mathbf{x}} + \text{h.c.}] , \quad (2)$$

where we include transverse (\pm) and longitudinal (L) polarizations in the sum. The creation and annihilation operators satisfy the commutation relations,

$$[a_\lambda(\vec{k}), a_\lambda^\dagger(\vec{k}')] = (2\pi)^3 \delta_{\lambda\lambda'} \delta^3(\vec{k} - \vec{k}') . \quad (3)$$

The scalar field and the vector mode functions, in Fourier space, will follow the equations of motion [16, 21]

$$\ddot{\phi} + 3H\dot{\phi} + V'(\phi) = \frac{\alpha}{4f}\langle F\tilde{F}\rangle, \quad (4)$$

$$\ddot{A}_\pm + H\dot{A}_\pm + \left(\frac{k^2}{a^2} \pm \frac{k}{a}\frac{\alpha\dot{\phi}}{f} + m^2\right)A_\pm = 0, \quad (5)$$

$$\ddot{A}_L + \frac{3k^2 + a^2m^2}{k^2 + a^2m^2}H\dot{A}_L + \left(\frac{k^2}{a^2} + m^2\right)A_L = 0. \quad (6)$$

The overdots denote derivatives with respect to physical time t and $k \equiv |k|$ is the magnitude of the comoving momentum. We consider only the spatially homogeneous zero momentum mode ($k = 0$) of the inflaton and have separated the three degrees of freedom of the vector into transverse and longitudinal components \bar{A}_T and A_L respectively, $\bar{k} \cdot \bar{A} = kA_L$ and $\bar{k} \cdot \bar{A}_T = 0$. Furthermore, we have written the transverse component in terms of the two helicities, $\bar{A}_T = \bar{\epsilon}_+ A_+ + \bar{\epsilon}_- A_-$.

Immediately, one observes how the inflaton motion enters into the equations of motion for the transverse modes. As for the longitudinal mode it is not affected by the presence of the coupling with the inflaton, nonetheless it may be produced via inflationary fluctuations, as described in [26].

We can write the transverse modes equation of motion in conformal time defined as $ad\tau = dt$,

$$\left[\frac{\partial^2}{\partial\tau^2} + k^2 \pm 2k\frac{\xi}{\tau}\right]A_\pm(k, \tau) = 0, \quad \xi \equiv \frac{\alpha\dot{\phi}}{2Hf} = \sqrt{\frac{\epsilon}{2}}\frac{\alpha}{f}m_{\text{P}}. \quad (7)$$

where $\tau \simeq -1/(aH)$ during inflation, and $\epsilon \equiv -\dot{H}/H^2$, which for single field inflation is given by

$$\epsilon \simeq \frac{\dot{\phi}^2}{2H^2m_{\text{Pl}}^2}. \quad (8)$$

Depending on the sign of the interaction parameter, ξ , one of the modes will experience tachyonic enhancement, when

$$k^2 \pm 2k\frac{\xi}{\tau} = k^2 \mp 2k\xi aH < 0. \quad (9)$$

Using the convention $\dot{\phi} > 0$, it results in $\xi > 0$, implying that only the A_+ mode will develop an instability, while A_- will stay in vacuum.

Treating ξ as constant, appropriate during a slow-roll evolution, and neglecting the vector mass one can solve Eq. (7) analytically in terms of Coulomb functions [48]. Under the tachyonic regime we are interested in, $-k\tau < 2\xi$ ($k < 2\xi aH$), and for $1/(8\xi) < -k\tau$ the WKB expansion provides a good approximation of the solution, giving a good intuition into the behavior of the modes around horizon crossing, when they experience the tachyonic enhancement [17, 21],

$$A_+(k, \tau)_{\text{WKB}} \simeq \frac{1}{\sqrt{2k}} \left(\frac{-k\tau}{2\xi}\right)^{1/4} e^{\pi\xi - 2\sqrt{-2\xi k\tau}}. \quad (10)$$

One may now study how the expression obtained in Eq. (10) behaves in comparison with numerical solutions of the system of equations.

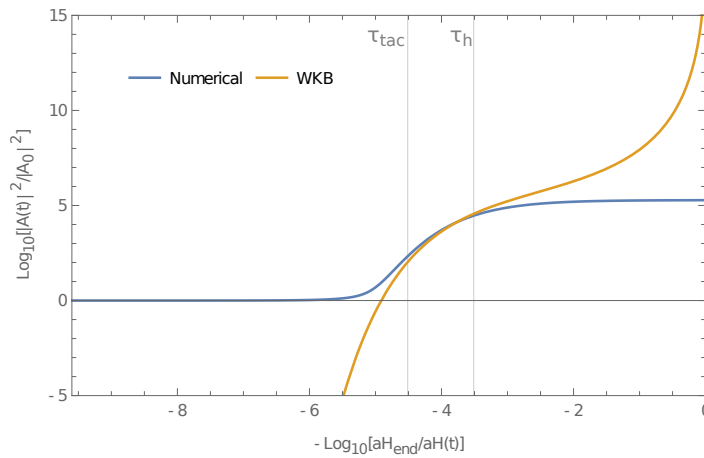


FIG. 1: Comparison of WKB Eq. (10), with the numerical solution for $|A_k|^2$ on LHS and $|A'_k|^2$ on RHS with $k \simeq 3 \times 10^{-5}(aH)_{end}$ and $\alpha/f = 11.5m_{PL}^{-1}$.

In Fig. 1, where we compare the vector mode amplitude evolution for both analytical, Eq. (10), and numerical solutions, we see that the WKB approximation describes well the time evolution during the tachyonic growth, but fails to describe the numerical results when the modes go out of the horizon. In regards to the numerical integration one obtains what is theoretically predicted, a three phase function: first in the vacuum state, then the tachyonic growth at $\tau_{tac} = -\xi/k$, to then almost freezing at the horizon crossing after $\tau_h \simeq -1/(10k)$.

With an aim of correctly describing the behavior of the gauge modes amplitudes and velocities, we build a semi-analytical solution. We combine the known analytical expressions in the vacuum state and the WKB solution during the tachyonic enhancement, with the amplitudes of A and A' at the end of inflation. Thus, from an arbitrary τ to τ_{end} , we use a step function that shall give

$$A_+(k, \tau) = \begin{cases} A_{BD}(k) & \tau < \tau_{tac} \\ A_{WKB}(k, \tau) & \tau_{tac} < \tau < \tau_h \\ A_+(k, \tau_{end}) & \tau > \tau_h \end{cases}, \quad (11)$$

with an analogous function for $A'_+(k, \tau)$. Finally, to obtain $A_+(k, \tau_{end})$ one must integrate the full numerical system for several modes k to obtain the spectrum at τ_{end} .

Recalling the inflaton equation of motion, on the right-hand side one has the backreaction of the gauge modes on the inflaton evolution

$$\ddot{\phi} + 3H\dot{\phi} + V'(\phi) = \frac{\alpha}{4f} \langle F\tilde{F} \rangle. \quad (12)$$

Typically backreaction effects are neglected if $\xi < \mathcal{O}(10)$ [33, 48], with ξ defined in Eq. (7). Moreover, ξ is constrained from the non-observation of non-gaussianities in CMB measurements to be $\lesssim 2.5$ [16, 17] at these scales (around 60 e-folds from the end of inflation). Naturally, this will constrain the coupling constant α/f . We then write ξ_{60} as the value of ξ at 60 e-folds before the end of inflation to fix such constants. In the case of slow-roll inflation with a quartic potential with no-backreaction ones has

$$\xi_{60} = 2 \frac{\alpha}{f} \frac{m_P^2}{\phi_{60}}. \quad (13)$$

Studying ξ evolution within the allowed parameter range one easily finds that from an initial non-backreacting regime the system evolves at the end of inflation to a relevant backreaction scenario, see Fig. 2. As expected from the proportionality with the inflaton velocity we get the maximum at the end of slow-roll inflation.

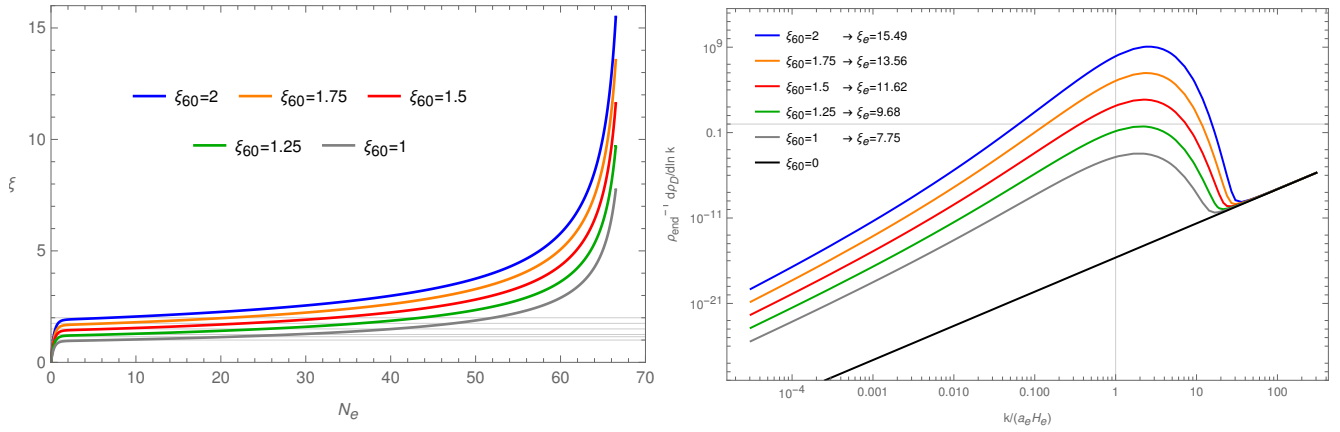


FIG. 2: Left panel: ξ evolution under no backreaction effects, we consider different values for the inflaton-vector coupling α/f , fixing ξ at 60 e-folds before the end of inflation as indicated in the plot. Right panel: Vector energy density spectrum normalized with the inflaton energy density at the end of inflation. The values for the interaction parameter at the end of inflation ξ_e are also indicated for each ξ_{60} .

In order to test if the system reaches a backreaction regime before the end of inflation, we may calculate the energy density spectrum for the vector modes ρ_A ,

$$\rho_A = \frac{1}{2} \langle \vec{E}^2 + \vec{B}^2 \rangle \quad (14)$$

$$= \frac{1}{4\pi^2 a^4} \int_0^\infty dk k^2 \left(|\partial_\tau A_+(k, \tau)|^2 + k^2 |A_+(k, \tau)|^2 \right) \quad (15)$$

$$= \frac{1}{2a^4} \int d \ln k \left(\mathcal{P}_{\partial_\tau A_+}(k, \tau) + k^2 \mathcal{P}_{A_+}(k, \tau) \right), \quad (16)$$

where we have neglected the subdominant contributions from A_- , and defined the power spectrum

$$\mathcal{P}_X(k, \tau) = \frac{k^3}{2\pi^2} |X(k, \tau)|^2 \quad X = A_+ \text{ or } \partial_\tau A_+, \quad (17)$$

with $\rho_A \equiv \langle \rho_A \rangle$ as the spacial average. Solving numerically for the equation of motion we can compute the quantity

$$\frac{1}{\rho_{end}} \frac{d\rho_A}{d \ln k} = \frac{1}{\rho_{end}} \frac{1}{2a^4} \left(\mathcal{P}_{\partial_\tau A_+}(k, \tau) + k^2 \mathcal{P}_{A_+}(k, \tau) \right) \quad (18)$$

at the end of inflation, where ρ_{end} corresponds to the total energy density in the universe. In a valid approximation, this ratio cannot be larger than one, i.e. the energy density of a single mode ought not to overcome the total energy density in the universe, here $\rho_{end} \simeq \rho_\phi$. The vector energy density spectrum at the end of inflation, normalized by the inflaton energy density, is shown on the RHS in Fig. 2. One can then see that already values of $\xi_{60} \geq 1.5$ will require taking into account backreaction effects to study gauge mode enhancement close to the end of inflation.

III. BACKREACTION ON THE INFLATON EVOLUTION

As seen in the previous section, from an initial non-backreacting dynamics at 60 e-folds, with the progression of slow-roll inflation the interaction parameter ξ will tend to grow into a backreacting regime. The equations of motion together with the Bianchi identities in terms of the electric and magnetic fields in conformal time are given by

$$\phi'' + 2aH\phi' - \nabla^2 \phi + a^2 \frac{dV(\phi)}{d\phi} = \frac{\alpha}{f} a^2 \vec{E} \cdot \vec{B}, \quad (19)$$

$$\vec{E}' + 2aH\vec{E} - \nabla \times \vec{B} = -\frac{\alpha}{f} \phi' \vec{B} - \frac{\alpha}{f} \vec{\nabla} \phi \times \vec{E}, \quad (20)$$

$$\vec{B}' + 2aH\vec{B} + \vec{\nabla} \times \vec{E} = 0, \quad (21)$$

$$\vec{\nabla} \cdot \vec{E} = -\frac{\alpha}{f} \vec{\nabla} \phi \cdot \vec{B} \quad (22)$$

$$\vec{\nabla} \cdot \vec{B} = 0, \quad (23)$$

with

$$a^2 \bar{B} = \bar{\nabla} \times \bar{A}, \quad (24)$$

$$a^2 \bar{E} = -\bar{A}' + a \bar{\nabla} A_0, \quad (25)$$

where ' denotes a derivative in conformal time τ . We now try a method to control the backreaction effects without relying on the WKB time derivative expansion, describing the electric contribution from the gauge modes. In essence we will rely on energy conservation of the vector modes, both longitudinal and transverse, to measure its impact on the background dynamics. The energy density evolution is given by

$$\dot{\rho}_\phi + 3H(\rho_\phi + p_\phi) = \dot{\phi} \frac{\alpha}{f} S_{EB}, \quad (26)$$

$$\dot{\rho}_A + 3H(\rho_A + p_A) = -\dot{\phi} \frac{\alpha}{f} S_{EB}, \quad (27)$$

with $S_{EB} = \langle \bar{E} \cdot \bar{B} \rangle$. Similarly one can study the source term

$$\dot{S}_{EB} = \dot{\bar{E}} \cdot \bar{B} + \bar{E} \cdot \dot{\bar{B}} = -4H\bar{E} \cdot \bar{B} - \frac{\alpha}{f} \dot{\phi} |\bar{B}|, \quad (28)$$

resulting in

$$\dot{S}_{EB} + 4HS_{EB} = -\frac{\alpha}{f} \dot{\phi} |\bar{B}|, \quad (29)$$

which composes a system of equations together with Eqs. (26) and (27) that only requires initial conditions and the input of the mean value of the magnetic field. We use the WKB approximation for the vector modes to estimate the later. Only the modes that suffer a tachyonic enhancement, $k < 2\xi aH$, become classical and can contribute to source the backreaction,

$$\langle |\bar{B}|^2 \rangle = \frac{1}{8\pi^3 a^4} \int d^3k k^2 \sum_{\lambda=\pm} |A_+|^2 \simeq \frac{e^{2\pi\xi}}{4\pi^2 a^4} \int dk k^3 \left(\frac{k}{2\xi aH} \right)^{1/2} e^{-4\sqrt{2\xi k/(aH)}} \simeq \frac{e^{2\pi\xi}}{\pi^2 \xi} \left(\frac{H}{64\xi} \right)^4 \times I[8\xi], \quad (30)$$

with

$$I[x] = 8! (1 - e^{-x}) - 8! e^{-x} \sum_{n=1}^8 \frac{x^n}{n!}. \quad (31)$$

Computing ξ with this new system of equations, and starting with the same initial conditions for the inflaton field than in Fig. 2, one now sees in Fig. 3 a flattening of the curves at the end of inflation when $\epsilon_H = 1$, leading to $\xi_e < 9$. In addition, one has some extra e-folds of inflation due to the slowing of the inflaton velocity. Therefore, in the case with backreaction, as we deviate from a pure single field slow-roll evolution, the definition for ξ_{60} Eq. (13) no longer holds. With the same inflaton initial conditions we now have a larger ξ_{60} than in a no-backreaction regime. Nonetheless, for the smaller initial interaction parameters $\xi_{60} \lesssim 1$ ($\alpha m_P/f \lesssim 11.5$) the difference can be neglected.

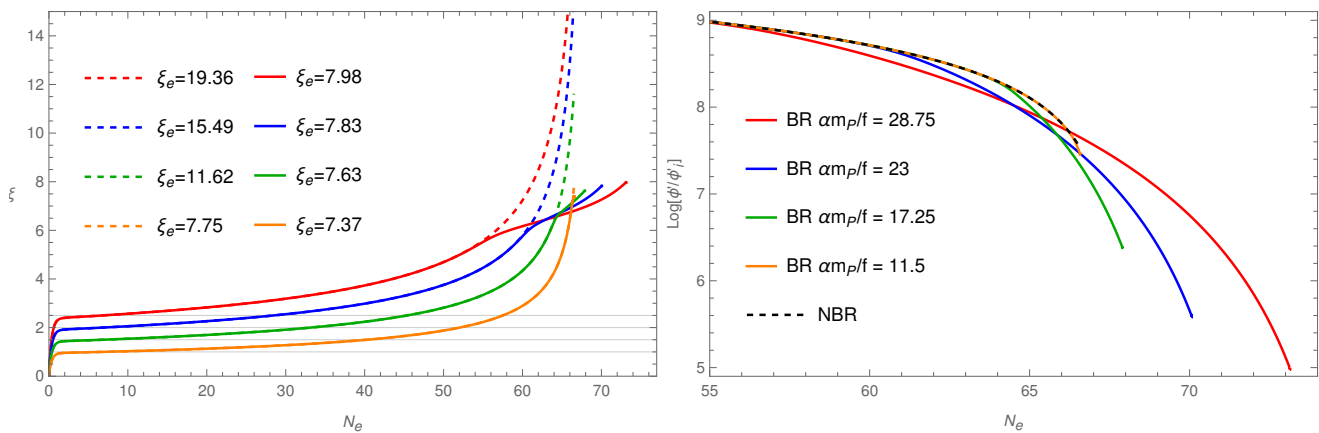


FIG. 3: Left panel: comparison of ξ evolution with (dashed) and without (solid) backreaction effects for $\alpha m_P/f = 28.75, 23, 17.25$ and 11.5 . Without backreaction, this gives respectively: $\xi_{60} = 2.5, 2, 1.5, 1$, at 60 e-folds. Right panel: we show the evolution of the inflaton velocity $\dot{\phi}$ normalized by its initial value for a slow-roll evolution. For no-backreaction (NBR) there is no dependence on ξ .

Although with a better picture in regards to the ξ parameter, and smaller values at the end of inflation ξ_e , we ought to compute again the spectral energy density to verify if the system maintains the correct energy balance. Normalizing this quantity with the total energy density, inflaton plus vector modes, we obtain the results shown on the LHS in Fig. 4. Solid lines give the spectrum at the end of inflation when $\epsilon_H = 1$, and for example for $\alpha m_P/f = 14.38$ the energy of the amplified vector modes will be larger than the total energy density in the universe, revealing that the backreaction effects are not still under control.

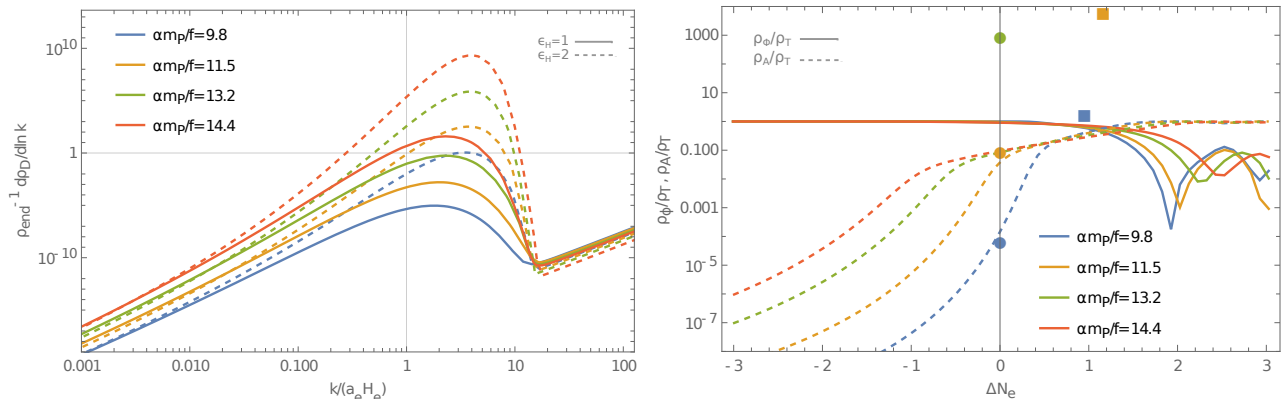


FIG. 4: Left panel: vector energy density spectrum normalized with the total energy density at the end of inflation, for different values of the inflaton-vector coupling α/f as indicated in the plot. In solid lines one has the spectrum at $\epsilon_H = 1$, whereas dashed lines are the result at $\epsilon_H = 2$. Right panel: evolution of the inflaton ρ_ϕ (solid lines) and vector ρ_A (dashed lines) energy densities, normalized by the total energy density $\rho_T = \rho_\phi + \rho_A$, as given by Eqs. (26) and (27). The no. of e-folds are counted with respect to the end of inflation, i.e., $\epsilon_H = 1$ when $\Delta N_e = 0$. Points marked with colored circles are the (approximated) numerical values of ρ_A obtained by integrating the spectrum shown on the LHS when $\epsilon_H = 1$, whereas the colored squares correspond to integration when $\epsilon_H = 2$.

The situation is direr if one takes into consideration the reheating transition, letting the system evolve until $\epsilon_H = 2$, dashed lines on the LHS in Fig. 4. Note that having an inflaton under a quartic potential, we have ensured a radiation-like stage after inflation, since the scalar field oscillating about the minimum redshifts as radiation. Although modes for which $k \gtrsim aH$ at $\epsilon_H = 1$ will remain inside the horizon, when analyzing the evolution, one realizes that there is still relevant amplitude growth until $\epsilon_H = 2$ for these modes that started to be amplified during the slow-roll regime. Thus, the parameter space where one can study gauge mode amplification with this system of backreaction equations is severely reduced, allowing only good estimates when $\alpha m_P/f \lesssim 9.78$, i.e. $\xi_{60} \lesssim 0.85$. This is also evident from the RHS in Fig. (4), where we show the evolution of the inflaton ρ_ϕ and vector ρ_A background energy densities with respect to the total energy density $\rho_T = \rho_\phi + \rho_A$, as given by Eqs. (26) and (27), for the same parameter values $\alpha m_P/f$ than on the LHS. N_e is the no. of e-folds, and $\Delta N_e = 0$ signal the end of inflation ($\epsilon_H = 1$) for all the curves. Here we have also included an estimation of ρ_A obtained by numerically integrating their spectral energy density over the relevant range of modes, when $\epsilon_H = 1, 2$ (colored circles and squares, respectively). Again, for example for $\alpha m_P/f = 13.2$ the spectrum obtained again is not consistent with the background evolution at $\epsilon_H = 1$. And although with $\alpha m_P/f = 11.5$ mode-by-mode integration is consistent up to $\epsilon_H = 1$, the amplification of vector modes continues and again at $\epsilon_H = 2$ we are off the background results by several orders of magnitude.

Indeed, what we have shown is that including BR effects only in the background evolution is not enough to capture the dynamics of the system near the end of inflaton and especially during the transition towards a radiation dominated universe, in particular that of the vector fluctuations. Even if we stay well within the linear regime when computing the evolution of the vector modes up to the end of inflation² ($\alpha m_P/f \lesssim 11.5$, $\xi_{60} \lesssim 1$), non-linearities are unavoidable during the transition towards $\epsilon_H = 2$, and these effects will set the final shape of the transverse modes spectrum.

Recently there have been interesting results in managing the backreaction of the vector modes on the inflaton evolution without requiring an integration and inclusion of the effects mode by mode, see [9, 45]. Nonetheless, no reheating has been included in these works. In a future work we hope to include a complete study for the gauge mode production. In regards to the present work, we will proceed with the numerical results obtained within the possible parameter space consistent with no BR up to $\epsilon_H = 2$ in order to calculate the full gravitational spectrum produced

² We notice that for $\alpha m_P/f \lesssim 11.5$ inflaton evolution does not change, and with or without BR the value of ξ_{60} is the same.

from the gauge modes amplification.

IV. POWER SPECTRUM GW'S

Here we study the production of gravitational waves induced by the electromagnetic modes. Focusing just on GW's we take the metric

$$ds^2 = a^2(\tau) [-d\tau^2 + (\delta_{ij} + h_{ij}) dx^i dx^j], \quad (32)$$

where $h^i_i = h_{ij,j} = 0$. The evolution of the tensor modes is given by

$$h''_{ij} + 2\frac{a'}{a}h'_{ij} - \Delta h_{ij} = \frac{2}{m_{\text{P}}^2}\Pi_{ij}{}^{lm}T_{lm}^{EM}, \quad (33)$$

where $\Pi_{ij}{}^{lm} = \Pi_l^i\Pi_m^j - \frac{1}{2}\Pi_{ij}\Pi^{lm}$ is the transverse traceless projector, with $\Pi_{ij} = \delta_{ij} - \partial_i\partial_j/\Delta$ and T_{lm}^{EM} contains the spacial contributions of the electromagnetic stress energy tensor. Now we change into a description in momentum space, projecting the tensor modes on the positive and negative-helicity solutions

$$h^{ij}(\mathbf{k}) = \sqrt{2} \sum_{\lambda=\pm} \epsilon_{\lambda}^i(\mathbf{k})\epsilon_{\lambda}^j(\mathbf{k})h_{\lambda}(\tau, \mathbf{k}), \quad (34)$$

and introduce the polarization tensors $\Pi_{\pm}^{ij}(\mathbf{k}) = \epsilon_{\mp}^i(\mathbf{k})\epsilon_{\mp}^j(\mathbf{k})/\sqrt{2}$, so that $h_{\pm}(\mathbf{k}) = \Pi_{\pm}^{ij}(\mathbf{k})h_{ij}(\mathbf{k})$. Using that $\Pi_{\pm}^{ij}\Pi_{ij}{}^{lm} = \Pi_{\pm}^{lm}$, the particular solution of Eq. (33) is given by

$$h_{\pm}(\mathbf{k}) = -\frac{2H^2}{m_{\text{P}}^2} \int d\tau' G_k(\tau, \tau') \tau'^2 \int \frac{d^3\mathbf{q}}{(2\pi)^3} \Pi_{\pm}^{lm}(\mathbf{k}) \times \\ \times [A'_l(\mathbf{q}, \tau') A'_m(\mathbf{k} - \mathbf{q}, \tau') - \varepsilon_{lab} q_a A_b(\mathbf{q}, \tau') \varepsilon_{mcd} (k - q)_c A_d(\mathbf{k} - \mathbf{q}, \tau')], \quad (35)$$

where $G_k(\tau, \tau')$ is the retarded Green function for the operator $d^2/d\tau^2 - (2/\tau)d/d\tau + k^2$,

$$G_k(\tau, \tau') = \frac{1}{k^3\tau'^2} [(1 + k^2\tau\tau') \sin k(\tau - \tau') + k(\tau' - \tau) \cos k(\tau - \tau')] | \quad (36)$$

for $\tau > \tau'$, while $G_k(\tau < \tau') = 0$.

We will be interested in promoting the gauge modes to operators, see Eq. (2), to then proceed with the tensor modes. As discussed in section II we will describe the vector mode amplitudes with a step function. In order to relate each stage to the amplitudes at the maximum, at the end of reheating, recovering Eq. (11), we write our step function for A_+ and A'_+ with the transfer functions T and \bar{T} as

$$A_+(k, \tau) = A_{end}(k) T^{\mathbf{k}}(\tau, \tau_{end}) \simeq \begin{cases} A_{BD}(k) & \tau < \tau_{tac} \\ A_{WKB}(k, \tau) & \tau_{tac} < \tau < \tau_h \\ A_{end}(k) & \tau > \tau_h \end{cases} \quad (37)$$

For the GW spectrum integration we have removed the Bunch-Davis vacuum contribution in the gauge amplitudes as it would introduce spurious contributions in the spectrum and we are interested in studying the tachyonic amplification effects. For the numerical computation we use the smooth functions

$$|A_{end}(k)|^2 T^{\mathbf{k}}(\tau, \tau_{end})^2 = \frac{|A_{WKB}(k, \tau)|^2}{2} \left[1 - \tanh\left(\delta\left(\frac{\tau}{\tau_h} - 1\right)\right) \right] \\ + \frac{|A_{end}(k)|^2}{2} \left[1 + \tanh\left(\delta\left(\frac{\tau}{\tau_h} - 1\right)\right) \right], \quad (38)$$

with $\delta = 10$, $\tau_{tac} = -\xi/k$ and $\tau_h = -1/(10k)$. An analogous description is used for $A'_+(k, \tau)$ with \bar{T} as the respective transfer function.

Furthermore, to describe the spectrum for $|A'_{end}(k)|^2$, $k^2|A_{end}(k)|^2$ and $k|AA'_{end}(k)|$ at $\epsilon_H = 2$, we use the functions in Eqs. (39), (40) and (41) which have a very good agreement with the numerically computed spectrums at the end of reheating (see Fig. 8 in Appendix A):

$$|A'_{end}(k)|^2 \simeq (a_e H_e) \exp \left[\left(x_0^{A'} + x_1^{A'} \tilde{k} + x_2^{A'} \tilde{k}^2 + x_3^{A'} \tilde{k}^3 \right) \left(1 - e^{a_0^{A'}(\tilde{k}-a_1^{A'})} \right) \right], \quad (39)$$

$$k^2|A_{end}(k)|^2 \simeq (a_e H_e) \exp \left[\left(x_0^A + x_1^A \tilde{k} + x_2^A \tilde{k}^2 + x_3^A \tilde{k}^3 \right) \left(1 - e^{a_0^A(\tilde{k}-a_1^A)} \right) \right], \quad (40)$$

$$k|AA'_{end}(k)| \simeq (a_e H_e) \exp \left[\left(x_0^{AA'} + x_1^{AA'} \tilde{k} + x_2^{AA'} \tilde{k}^2 + x_3^{AA'} \tilde{k}^3 \right) \left(1 - e^{a_0^{AA'}(\tilde{k}-a_1^{AA'})} \right) \right], \quad (41)$$

with $\tilde{k} = k/(a_e H_e)$ and where the x 's and a 's are functions of ξ_{60} listed in Appendix A. Setting $A_- = 0$ we calculate the two point function for the gravitational waves as described in detail in Appendix B. Taking $x = -k\tau$ and $\tilde{q} = q/(a_e H_e)$ we get

$$\begin{aligned} \langle h_s h_{s'} \rangle &= \frac{2}{(2\pi)^3} \frac{H^4}{m_P^4} \frac{(a_e H_e)^5}{k^8} \int_0^\infty \int_0^\infty dx_1 dx_2 (\sin x_1 - x_1 \cos x_1) (\sin x_2 - x_2 \cos x_2) \\ &\int_0^\infty d\tilde{q} \int_0^{2\pi} \frac{2\pi}{16} \tilde{q}^2 d\theta (1 + s \cos \theta) (1 + s' \cos \theta) \left(1 + s \frac{1 - \frac{\tilde{q} \cos \theta}{k}}{\sqrt{1 + \frac{\tilde{q}^2}{k^2} - 2\frac{\tilde{q}}{k} \cos \theta}} \right) \left(1 + s' \frac{1 - \frac{\tilde{q} \cos \theta}{k}}{\sqrt{1 + \frac{\tilde{q}^2}{k^2} - 2\frac{\tilde{q}}{k} \cos \theta}} \right) \\ &(\tilde{q}^2(\tilde{k} - \tilde{q})^2 |A_{end}(\tilde{q})|^2 |A_{end}(\tilde{k} - \tilde{q})|^2 T_{\tilde{q}}^{x_1} T_{\tilde{q}}^{x_2} T_{\tilde{k}-\tilde{q}}^{x_1} T_{\tilde{k}-\tilde{q}}^{x_2} \\ &+ |A'_{end}(\tilde{q})|^2 |A'_{end}(\tilde{k} - \tilde{q})|^2 \bar{T}_{\tilde{q}}^{x_1} \bar{T}_{\tilde{q}}^{x_2} \bar{T}_{\tilde{k}-\tilde{q}}^{x_1} \bar{T}_{\tilde{k}-\tilde{q}}^{x_2} \\ &+ \tilde{q}(\tilde{k} - \tilde{q}) |AA'_{end}(\tilde{q})| |AA'_{end}(\tilde{k} - \tilde{q})| (T_{\tilde{q}}^{x_1} \bar{T}_{\tilde{q}}^{x_2} T_{\tilde{k}-\tilde{q}}^{x_1} \bar{T}_{\tilde{k}-\tilde{q}}^{x_2} + T_{\tilde{q}}^{x_2} \bar{T}_{\tilde{q}}^{x_1} T_{\tilde{k}-\tilde{q}}^{x_2} \bar{T}_{\tilde{k}-\tilde{q}}^{x_1})). \end{aligned} \quad (42)$$

From the correlation functions we obtain the power spectrum that is then related to the fraction of energy density of gravitational waves today by [49, 50]

$$\Omega_{ss'} h^2 = \frac{\Omega_{R0} h^2}{24} \frac{k^3}{2\pi^2} \langle h_s h_{s'} \rangle, \quad (43)$$

where $\Omega_{R0} h^2 \equiv \rho_{R0} h^2 / 3H_0^2 m_P^2 \simeq 4.18 \times 10^{-5}$. Finally the dependence in k is related to frequency today by

$$f = \frac{k}{2\pi a_0} = \frac{\tilde{k}}{2\pi} H_e \frac{a_e}{a_0}, \quad (44)$$

with $\tilde{k} = k/(a_e H_e)$. In Fig. 5 we represent the spectral energy density of the induced gravitational waves from Eq. (43) for both $s = s' = +$ (solid lines) and $s = s' = -$ (dashed lines), and several values of ξ_{60} . The BBN limit, $\Omega_{GW} h^2 < 1.8 \times 10^{-6}$, that sets an upper bound on the radiation excess at BBN, and the sensitivity curves for planned GW detectors are also included [15, 51]. We find a parity asymmetric spectrum with a difference at the peaks of 2/3 orders of magnitude between the $++$ and $--$ correlations, in line with the results obtained at CMB scales in [12, 14, 15]. The peaks for the spectral distribution come around 10^7 Hz, typical in end of inflation and (p)reheating stages, exactly where we had the maximum spectral amplification for the vector modes. At larger frequencies the spectrum falls exponentially, again following the effects of the electromagnetic sources with a correct vacuum subtraction [52]. In the range of frequencies where one could have a detection of the represented signals there are no current or planned GW detectors, although interesting proposals are discussed in [53–55]. At present and planned interferometer scales the energy densities are small for the interaction parameters ξ we were able to consider. For $\xi_{60} = 1$ ($\alpha m_P / f = 11.5$), a parameter already beyond the linear backreaction treatment that we have employed as discussed in section III, we obtain a energy density that surpasses the BBN bound. This does not exclude models with this or larger couplings, only reveals the need for an appropriate description of the vector mode amplification, fully including non-linearities in the evolution. The GW spectrum going beyond the linear regime remains to be calculated.

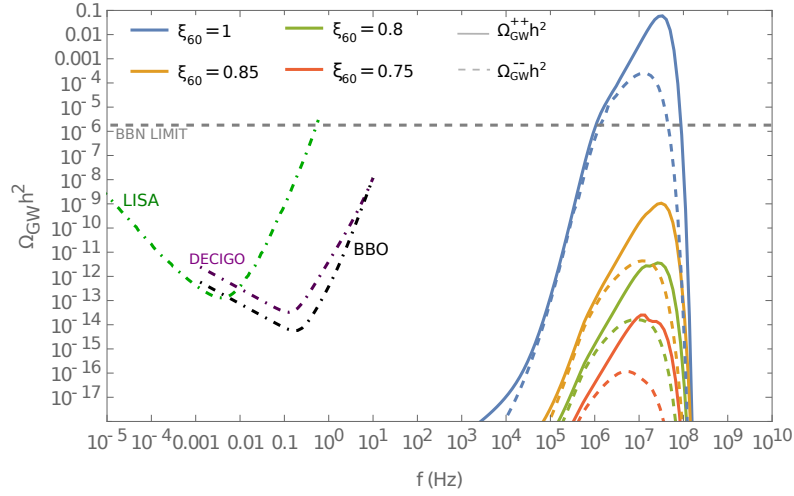


FIG. 5: Spectral density of GW's in frequency today sourced by the tachyonic amplification of vector modes. Sensitivity curves for LISA, DECIGO and BBO are included as well as the BBN energy density limit.

We now compare, in Fig. 6, our results with the expressions obtained in [15], following the work in [12], where the analytic expression in Eq. (10) was employed on the two point correlation function.

$$\Omega_{++}^{WKB} h^2 \simeq 1.5 \times 10^{-13} \frac{H^4}{m_P^4} \frac{e^{4\pi\xi}}{\xi^6}, \quad (45)$$

$$\Omega_{--}^{WKB} h^2 \simeq 3.1 \times 10^{-16} \frac{H^4}{m_P^4} \frac{e^{4\pi\xi}}{\xi^6}. \quad (46)$$

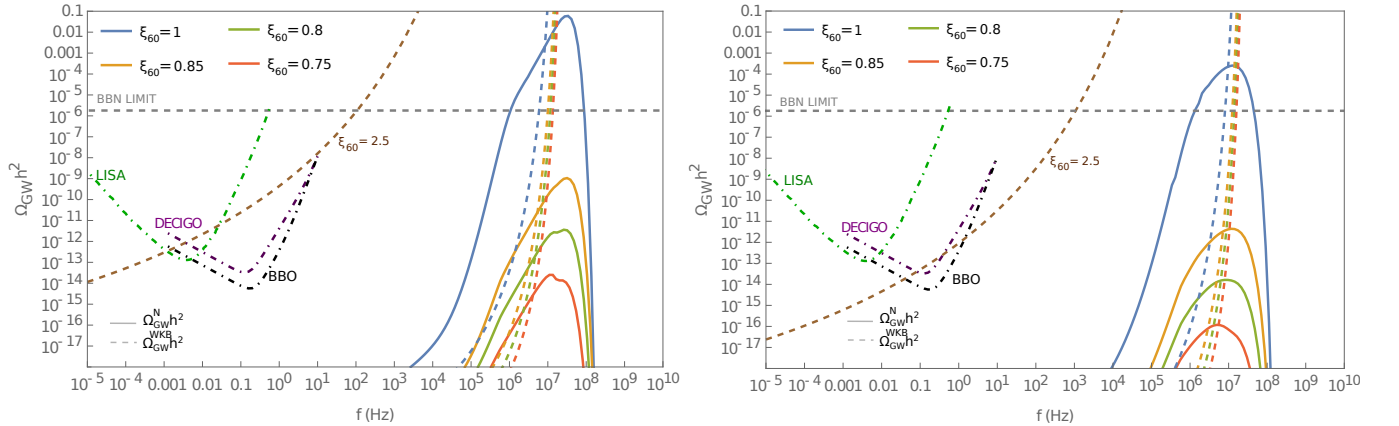


FIG. 6: Comparison of the spectral energy density for the GW's produced from the tachyonic amplification estimated by the semi analytical method described with Eqs. (42) and (43), and the analytical description with the WKB solution for the vector modes Eqs. (46) and (45). In the left panel we show the $++$ two point function and in the right panel the $--$ correlation.

The shortcomings of the analytical estimations with the WKB expansion are apparent in Fig. 6. With the expressions in Eqs. (46) and (45) one may get appropriate descriptions at CMB scales, allowing for instance the study of parity violating signals in the B-modes [12]. However, at frequencies typical of end of inflation (MHz) the expressions become less reliable as we are no longer in the constant ξ regime and the deviations from our curves are substantial. Furthermore, for an interaction parameter $\xi_{60} \simeq 2.5$ as was considered in [15], the linear description no longer holds and the estimation for a detection with LISA is a stretch for the model capabilities. Nonetheless, as the non-linear dynamics present with strong backreaction remains to be integrated in the GW spectrum calculation, the possibility may be dim but it is not excluded.

Finally, we can combine the numerical procedure to obtain the energy density of the gravitational waves today, where we use the amplitude spectrum of the gauge modes contributions through Eqs. (40), (39) and (41), and the

upper bound on the radiation excess at BBN to set an estimate of a ceiling on the amplitude of such electromagnetic sources. As each individual contribution, from $|A'|^2$, $k^2|A|^2$ and $k|A'A|$, are of similar order, through a simple linear fit we find the would be maximum amplitude of the electric contribution $|A'|^2$, our representative, to reach the BBN bound, see figure 7. We obtain a maximum amplitude at $|A'|^2 \simeq 1.42 \times 10^{16} a_e H_e$.

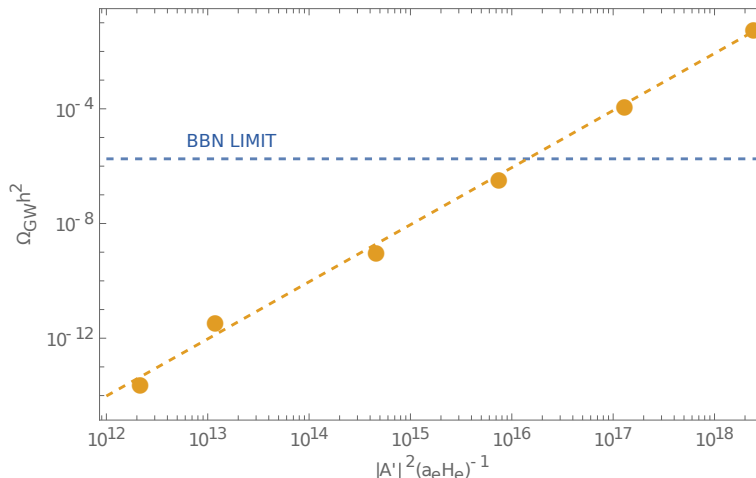


FIG. 7: Linear interpolation to obtain the maximum amplitude on the electric field contribution $|A'|^2$. The points to obtain the linear fit were obtained using (from left to right) $\xi_{60} = 0.75, 0.8, 0.85, 0.9, 0.95$ and 1 at 60 e-folds.

Note that this analysis is independent of a correct or incorrect parametrization of the backreaction effects on the inflaton evolution. The assumption is that the gauge modes spectrum will keep a similar shape, where the main contribution for the integration in Eq. (42) comes through a dominant peak for the modes amplified close to the end of inflation as in the amplitudes represented in figure 8.

V. CONCLUSION

In this work we have calculated the gravitational wave spectrum produced from the "axionlike" interaction between the inflaton and an $U(1)$ gauge field, in the linear regime during inflation and reheating. Main results are presented in figure 5.

During the slow-roll evolution, the inflaton motion sources a tachyonic amplification of the gauge field amplitudes. From the asymmetry present in the $\phi F \tilde{F}$ interactions, only one of the transverse polarizations is amplified resulting in a parity asymmetric source for the gravitational waves. Naturally this propagates into the GW spectrum as seen in Fig. 5 and predicted when contrasting Eqs. (45) and (46). The peaks in the GW spectrum appear around 10^7 Hz, as expected from the maximal amplification of the vector modes at the end of inflation and reheating. We have also shown an example with $\xi_{60} \simeq 1$ ($\alpha/f \simeq 11.5 m_P^{-1}$), where computing a spectrum with a slightly inadequate description could point to an erroneous exclusion of a parameter space due to a crossing into the BBN limit on the GW energy density. The analytical predictions obtained with the WKB solution Eqs. (45) and (46) vary significantly from our curves at large frequencies, as seen in Fig. 6. The prediction of a detection with LISA obtained for $\xi_{60} \simeq 2.5$ ($\alpha m_P/f \simeq 28.75$) goes beyond the validity of the WKB analytical description. Nevertheless, a signal within the detector sensitivity may come as a combination of the undescribed non-linear dynamics in the strong backreaction regime and a low scale inflation model compatible with the observations³. At the large frequencies ranges (MHz) predicted in our calculations there are no planned or expected detectors. We thus hope that this work motivates proposals and further development of ideas to detect signals within this regime where there are no known astrophysical sources.

To derive the GW spectrum we have studied the vector production until the end of reheating when the tachyonic amplification comes to a halt. The gauge field amplitudes are described with a smoothed step function, initially with the analytical WKB solution, and after horizon crossing with the amplitudes value at $\epsilon_H = 2$, obtained through the

³ For instance, with the potential in [56] one can lower inflation scale enough to generate a peak around Hz scale. Moreover, as showed in [33], the shape of the potential will not modify the shape in the electromagnetic spectrum.

numerical integration of the equations of motion. Therein we combine the good estimation in the WKB solution for the start of the tachyonic enhancement with an almost constant amplitude from the horizon crossing of the modes until the end of the inflationary dynamics. Here we have considered a simple system to attempt to mimic the backreaction effects on the inflationary motion based on energy conservation on the vector modes. We were then able to reproduce the vector production with the correct description for $\xi_{60} \lesssim 0.85$ ($\alpha m_P/f \lesssim 9.78$). Furthermore, we have obtained an estimation of the upper bound on the amplitudes of the electromagnetic sources, $k^2|A|^2$, $|A'|^2$, $k|A'A|$. In order to avoid radiation excess at BBN one has to verify $|A'|^2 < 1.42 \times 10^{16} a_e H_e$.

In order to extend the parameter space to the constrains given by the upper bound on non-Gaussianities, $\xi_{60} \simeq 2.5$ ($\alpha m_P/f \simeq 28.75$), the non-linear dynamics of the backreaction effects have to be integrated in the system. With the gradient expansion formalism, through a system of 3-n differential equations for bilinear functions of the electromagnetic fields in coordinate space, the authors of [9] were able to manage those effects until the end of inflation, $\epsilon_H = 1$. The oscillating effects in the ξ evolution close to the end of inflation, also confirmed in the works [8, 10], seem to induce a double peak in the gauge particle amplitudes spectrum that could result in interesting effects on the GW spectrum.

As future a direction of this work we will be looking for a correct estimation of vector production in the strong backreaction case both during inflation and until the end of reheating, at $\epsilon_H = 2$. To then estimate the gravitational wave spectrum in the entirety of the allowed parameter range. It would also be interesting to study if the GW spectrum exhibits non-Gaussian statistics inducing a more distinct signal on a possible detection.

Appendix A: Spectrum for E^2 , B^2 and $E \cdot B$

We present here how we modeled the parameters in the functions in Eqs. (39), (40) and (41) in terms of ξ_{60} , i.e., the value of the interacting parameter ξ 60 e-folds before the end of inflation. Recall that for values $\xi_{60} \lesssim 1$ the field background evolution is not modified, and the definition (13) holds. And in Fig. (8) we compared our semi-analytical parametrization with the spectrum obtained numerically for the amplitudes of $a^4 E^2$, $a^4 B^2$ and $a^4 E \cdot B$.

$$x_0^{A'}(\xi_{60}) = -6.06884 + 43.8484 \xi_{60} \quad (\text{A1})$$

$$x_1^{A'}(\xi_{60}) = -2.57099 + 7.69049 \xi_{60} \quad (\text{A2})$$

$$x_2^{A'}(\xi_{60}) = -0.185844 + 0.689615 \xi_{60} \quad (\text{A3})$$

$$x_3^{A'}(\xi_{60}) = -0.00704665 + 0.0222908 \xi_{60} \quad (\text{A4})$$

$$a_0^{A'}(\xi_{60}) = 0.650179 - 0.661859 \xi_{60} \quad (\text{A5})$$

$$a_1^{A'}(\xi_{60}) = 1.49961 - 1.33578 \xi_{60} \quad (\text{A6})$$

$$x_0^A(\xi_{60}) = -2.96245 + 42.6144 \xi_{60} \quad (\text{A7})$$

$$x_1^A(\xi_{60}) = -1.44173 + 7.13583 \xi_{60} \quad (\text{A8})$$

$$x_2^A(\xi_{60}) = -0.30357 + 0.745283 \xi_{60} \quad (\text{A9})$$

$$x_3^A(\xi_{60}) = -0.013457 + 0.029614 \xi_{60} \quad (\text{A10})$$

$$a_0^A(\xi_{60}) = 0.444126 + 0.979801 \xi_{60} \quad (\text{A11})$$

$$a_1^A(\xi_{60}) = 1.90892 + 0.883274 \xi_{60} \quad (\text{A12})$$

$$x_0^{AA'}(\xi_{60}) = -3.39633 + 41.8843 \xi_{60} \quad (\text{A13})$$

$$x_1^{AA'}(\xi_{60}) = -0.413385 + 6.69622 \xi_{60} \quad (\text{A14})$$

$$x_2^{AA'}(\xi_{60}) = -0.149098 + 0.60052 \xi_{60} \quad (\text{A15})$$

$$x_3^{AA'}(\xi_{60}) = -0.00542463 + 0.0199417 \xi_{60} \quad (\text{A16})$$

$$a_0^{AA'}(\xi_{60}) = 0.233569 + 1.17342 \xi_{60} \quad (\text{A17})$$

$$a_1^{AA'}(\xi_{60}) = 1.97323 + 0.850476 \xi_{60} \quad (\text{A18})$$

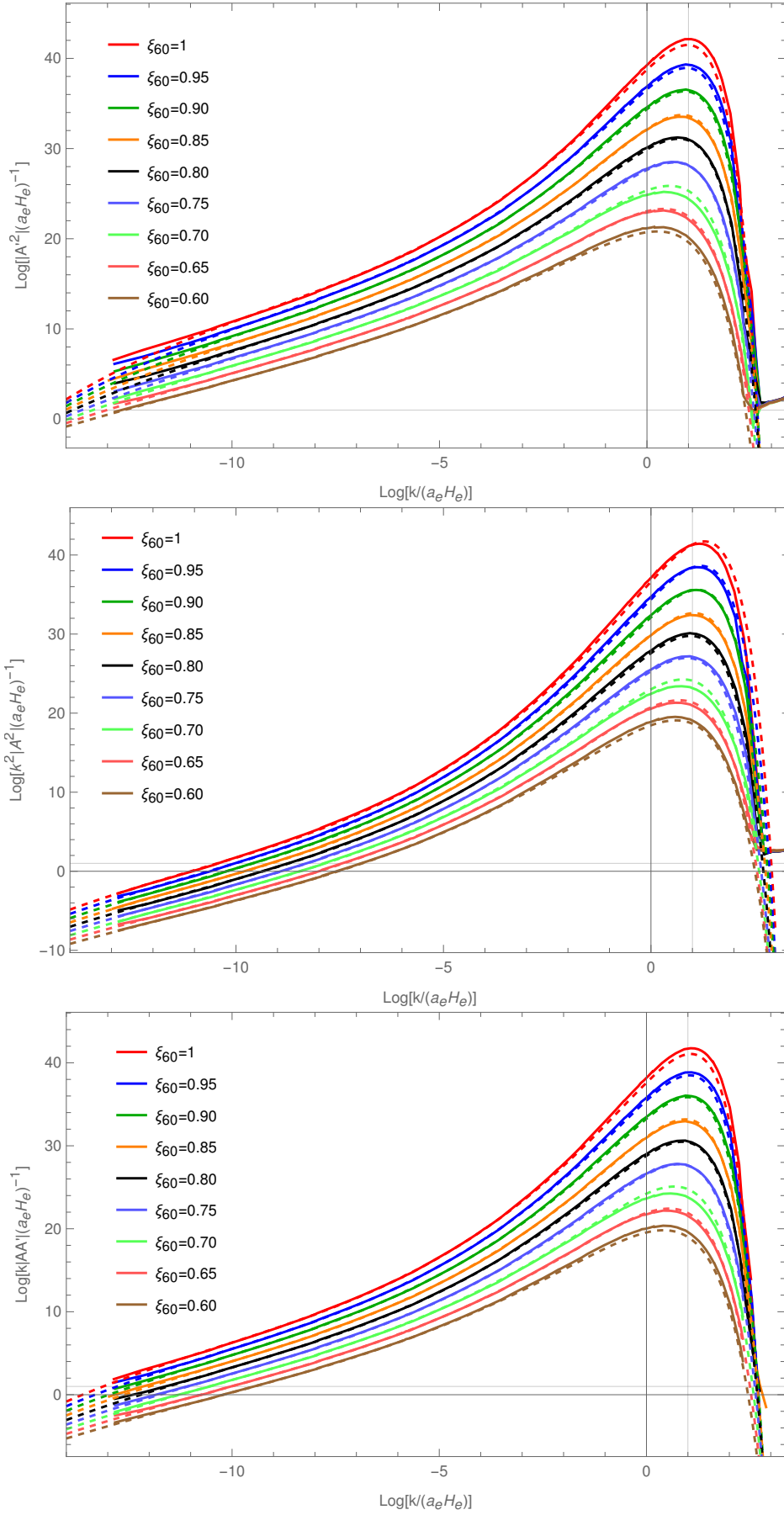


FIG. 8: Spectrum for E^2 , B^2 and $E \cdot B$ contributions at $\epsilon_H = 2$ compared to functions in Eqs. (39), (40) and (41), respectively. We have considered different values for the inflaton-vector coupling α/f , fixing ξ at 60 e-folds.

Appendix B: Details on $\langle h_s h_{s'} \rangle$

We want to calculate the two point functions trying to keep the result in terms of the amplitude solutions for the gauge field modes at the end of inflation. Let us recover the vector mode expansion

$$\hat{A}_i(\tau, \mathbf{x}) = \int \frac{d^3 \mathbf{k}}{(2\pi)^3} e^{i\mathbf{k}\cdot\mathbf{x}} \hat{A}_i(\tau, \mathbf{k}) = \sum_{\lambda=\pm} \int \frac{d^3 \mathbf{k}}{(2\pi)^3} [\epsilon_\lambda^i(\mathbf{k}) A_\lambda(\tau, \mathbf{k}) \hat{a}_\lambda^{\mathbf{k}} e^{i\mathbf{k}\cdot\mathbf{x}} + \text{h.c.}] \quad (\text{B1})$$

where $\hat{a}_\lambda^{\mathbf{k}}, \hat{a}_\lambda^{\mathbf{k}\dagger}$ are the annihilation and creation operators. Now, we promote the tensor modes to operators

$$\begin{aligned} \hat{h}_\pm(\mathbf{k}) &= -\frac{2H^2}{\sqrt{2}m_P^2} \int d\tau' G_k(\tau, \tau') \tau'^2 \int \frac{d^3 \mathbf{q}}{(2\pi)^3} \times \\ &\times \left[\hat{\mathcal{A}}'_{\pm, \lambda}(\mathbf{k}, \mathbf{q}, \tau') \hat{\mathcal{A}}'_{\pm, \lambda'}(\mathbf{k}, \mathbf{k} - \mathbf{q}, \tau') - \varepsilon_{lab} q_a \hat{\mathcal{A}}_{\pm, \lambda}(\mathbf{k}, \mathbf{q}, \tau') \varepsilon_{mcd} (k - q)_c \hat{\mathcal{A}}_{\pm, \lambda'}(\mathbf{k}, \mathbf{k} - \mathbf{q}, \tau') \right] \quad (\text{B2}) \\ &= -\frac{2H^2}{\sqrt{2}m_P^2} \int d\tau' G_k(\tau, \tau') \tau'^2 \int \frac{d^3 \mathbf{q}}{(2\pi)^3} \times \\ &\sum_{\lambda, \lambda'=\pm} [(\epsilon_\mp^l(\mathbf{k}) \epsilon_\lambda^l(\mathbf{q}) A'_\lambda(\mathbf{q}, \tau') \hat{a}_\lambda^{\mathbf{k}} + \text{h.c.}) (\epsilon_\mp^m(\mathbf{k}) \epsilon_{\lambda'}^m(\mathbf{k} - \mathbf{q}) A'_{\lambda'}(\mathbf{k} - \mathbf{q}, \tau') \hat{a}_{\lambda'}^{\mathbf{k}} + \text{h.c.}) \\ &- (-\lambda)(-\lambda') i^2 q |k - q| (\epsilon_\mp^l(\mathbf{k}) \epsilon_\lambda^l(\mathbf{q}) A_\lambda(\mathbf{q}, \tau') \hat{a}_\lambda^{\mathbf{k}} + \text{h.c.}) (\epsilon_\mp^m(\mathbf{k}) \epsilon_{\lambda'}^m(\mathbf{k} - \mathbf{q}) A_{\lambda'}(\mathbf{k} - \mathbf{q}, \tau') \hat{a}_{\lambda'}^{\mathbf{k}} + \text{h.c.})] \quad (\text{B3}) \end{aligned}$$

where $\hat{\mathcal{A}}_{s, \lambda}(\mathbf{k}, \mathbf{q}, \tau') = \epsilon_{-s}^l(\mathbf{k}) \epsilon_\lambda^l(\mathbf{q}) A_\lambda(\mathbf{q}, \tau') \hat{a}_\lambda^{\mathbf{k}}$, we have used $\varepsilon_{abc} k_b \epsilon_\lambda^c = -\lambda i k \epsilon_\lambda^a$ and decomposed $\Pi_\pm^{lm}(\mathbf{k})$. Now, to calculate the two point function we may use Wick's theorem to simplify our expression, the only non zero terms will be given by $\langle \hat{c}_\lambda^{\mathbf{k}} \hat{c}_{\lambda'}^{\mathbf{k}\dagger} \rangle = (2\pi)^3 \delta(\mathbf{k} - \mathbf{k}') \delta_{\lambda\lambda'}$ contributions

$$\begin{aligned} \langle h_s(\mathbf{k}) h_{s'}(\mathbf{k}') \rangle &= 2 \frac{H^4}{m_P^4} \int d\tau' d\tau'' \tau'^2 \tau''^2 G_k(\tau, \tau') G_k(\tau, \tau'') \int \frac{d^3 \mathbf{q}}{(2\pi)^3} \int \frac{d^3 \mathbf{q}'}{(2\pi)^3} \sum_{\lambda, \lambda', \Lambda, \Lambda'}^\pm \\ &\langle [\epsilon_{-s}^l(\mathbf{k}) \epsilon_\lambda^l(\mathbf{q}) \epsilon_{-s'}^m(\mathbf{k}) \epsilon_{\lambda'}^m(\mathbf{k} - \mathbf{q}) A'_\lambda(\mathbf{q}, \tau') A'_{\lambda'}(\mathbf{k} - \mathbf{q}, \tau') \hat{a}_\lambda^{\mathbf{q}} \hat{a}_{\lambda'}^{\mathbf{k} - \mathbf{q}} \\ &+ \lambda \lambda' q (k - q) \epsilon_{-s}^l(\mathbf{k}) \epsilon_\lambda^l(\mathbf{q}) \epsilon_{-s'}^m(\mathbf{k}) \epsilon_{\lambda'}^m(\mathbf{k} - \mathbf{q}) A_\lambda(\mathbf{q}, \tau') A_{\lambda'}(\mathbf{k} - \mathbf{q}, \tau') \hat{a}_\lambda^{\mathbf{q}} \hat{a}_{\lambda'}^{\mathbf{k} - \mathbf{q}}] \\ &[\epsilon_{-s}^{*a}(\mathbf{k}') \epsilon_{\Lambda}^{*a}(\mathbf{q}') \epsilon_{-s'}^{*b}(\mathbf{k}') \epsilon_{\Lambda'}^{*b}(\mathbf{k}' - \mathbf{q}') A_{\Lambda}^*(\mathbf{q}', \tau'') A_{\Lambda'}^*(\mathbf{k}' - \mathbf{q}', \tau'') \hat{a}_{\Lambda}^{\dagger \mathbf{q}'} \hat{a}_{\Lambda'}^{\dagger \mathbf{k}' - \mathbf{q}'} \\ &+ \Lambda \Lambda' q' (k' - q') \epsilon_{-s}^{*a}(\mathbf{k}') \epsilon_{\Lambda}^{*a}(\mathbf{q}') \epsilon_{-s'}^{*b}(\mathbf{k}') \epsilon_{\Lambda'}^{*b}(\mathbf{k}' - \mathbf{q}') A_{\Lambda}^*(\mathbf{q}', \tau'') A_{\Lambda'}^*(\mathbf{k}' - \mathbf{q}', \tau'') \hat{a}_{\Lambda}^{\dagger \mathbf{q}'} \hat{a}_{\Lambda'}^{\dagger \mathbf{k}' - \mathbf{q}'}] \rangle \quad (\text{B4}) \end{aligned}$$

with the relations on $\langle \hat{a}_\lambda^{\mathbf{q}} \hat{a}_{\lambda'}^{\mathbf{k} - \mathbf{q}} \hat{a}_{\Lambda}^{\dagger \mathbf{q}'} \hat{a}_{\Lambda'}^{\dagger \mathbf{k}' - \mathbf{q}'} \rangle$ the two point function can be simplified into

$$\begin{aligned} \langle h_s(\mathbf{k}) h_{s'}(\mathbf{k}') \rangle &= \frac{2}{(2\pi)^3} \frac{H^4}{m_P^4} \delta(\mathbf{k} + \mathbf{k}') \int d\tau' d\tau'' \tau'^2 \tau''^2 G_k(\tau, \tau') G_k(\tau, \tau'') \\ &\int d^3 \mathbf{q} \sum_{\lambda, \lambda'}^\pm \epsilon_{-s}^l(\mathbf{k}) \epsilon_\lambda^l(\mathbf{q}) \epsilon_{-s}^m(\mathbf{k}) \epsilon_{\lambda'}^m(\mathbf{k} - \mathbf{q}) \epsilon_{-s'}^{*a}(\mathbf{k}) \epsilon_{\lambda'}^{*a}(\mathbf{q}) \epsilon_{-s'}^{*b}(\mathbf{k}) \epsilon_{\lambda'}^{*b}(\mathbf{k} - \mathbf{q}) \\ &\times [A'_\lambda(\mathbf{q}, \tau') A'_{\lambda'}(\mathbf{k} - \mathbf{q}, \tau') + \lambda \lambda' q (k - q) A_\lambda(\mathbf{q}, \tau') A_{\lambda'}(\mathbf{k} - \mathbf{q}, \tau')] \\ &\times [A_{\lambda}^*(\mathbf{q}, \tau'') A_{\lambda'}^*(\mathbf{k} - \mathbf{q}, \tau'') + \lambda \lambda' q (k - q) A_{\lambda}^*(\mathbf{q}, \tau'') A_{\lambda'}^*(\mathbf{k} - \mathbf{q}, \tau'')]. \quad (\text{B5}) \end{aligned}$$

As studied for the cosmological evolution during inflation, the gauge modes with + helicity will be severely amplified and the negative solution will be suppressed. Taking $A_- \simeq 0$ we find

$$\begin{aligned} \langle h_s(\mathbf{k}) h_{s'}(\mathbf{k}') \rangle &= \frac{2}{(2\pi)^3} \frac{H^4}{m_P^4} \delta(\mathbf{k} + \mathbf{k}') \int d\tau' d\tau'' \tau'^2 \tau''^2 G_k(\tau, \tau') G_k(\tau, \tau'') \\ &\int d^3 \mathbf{q} \epsilon_{-s}^l(\mathbf{k}) \epsilon_+^l(\mathbf{q}) \epsilon_{-s}^{*a}(\mathbf{k}) \epsilon_+^{*a}(\mathbf{q}) \epsilon_{-s}^m(\mathbf{k}) \epsilon_+^m(\mathbf{k} - \mathbf{q}) \epsilon_{-s'}^{*b}(\mathbf{k}) \epsilon_+^{*b}(\mathbf{k} - \mathbf{q}) \times \quad (\text{B6}) \\ &\{ A'_+(\mathbf{q}, \tau') A'_+(\mathbf{k} - \mathbf{q}, \tau') A_+^*(\mathbf{q}, \tau'') A_+^*(\mathbf{k} - \mathbf{q}, \tau'') + q^2 (k - q)^2 A_+(\mathbf{q}, \tau') A_+(\mathbf{k} - \mathbf{q}, \tau') A_+^*(\mathbf{q}, \tau'') A_+^*(\mathbf{k} - \mathbf{q}, \tau'') \\ &+ q(k - q) [A_+(\mathbf{q}, \tau') A_+(\mathbf{k} - \mathbf{q}, \tau') A_+^*(\mathbf{q}, \tau'') A_+^*(\mathbf{k} - \mathbf{q}, \tau'') + A'_+(\mathbf{q}, \tau') A'_+(\mathbf{k} - \mathbf{q}, \tau') A_+^*(\mathbf{q}, \tau'') A_+^*(\mathbf{k} - \mathbf{q}, \tau'')] \}. \end{aligned}$$

Assuming $A_+(\mathbf{q}, \tau') = A_+(\mathbf{q}, \tau) T(\mathbf{q}, \tau, \tau') = A_+^\tau(\mathbf{q}) T_{\tau, \tau'}^\mathbf{q}$, and $A'_+(\mathbf{q}, \tau') = A'_+(\mathbf{q}, \tau) \bar{T}(\mathbf{q}, \tau, \tau') = A'_+\tau(\mathbf{q}) \bar{T}_{\tau, \tau'}^\mathbf{q}$, where T and \bar{T} are real functions. We can then write

$$\begin{aligned} \langle h_s(\mathbf{k}) h_{s'}(\mathbf{k}') \rangle &= \frac{2}{(2\pi)^3} \frac{H^4}{m_P^4} \delta(\mathbf{k} + \mathbf{k}') \int d\tau' d\tau'' \tau'^2 \tau''^2 G_k(\tau, \tau') G_k(\tau, \tau'') \\ &\int d^3\mathbf{q} \epsilon_{-s}^l(\mathbf{k}) \epsilon_+^l(\mathbf{q}) \epsilon_{-s'}^{*a}(\mathbf{k}) \epsilon_+^{*a}(\mathbf{q}) \epsilon_{-s}^m(\mathbf{k}) \epsilon_+^m(\mathbf{k} - \mathbf{q}) \epsilon_{-s'}^{*b}(\mathbf{k}) \epsilon_+^{*b}(\mathbf{k} - \mathbf{q}) \times \\ &\left\{ |A'_+(\mathbf{q}, \tau')|^2 |A'_+(\mathbf{k} - \mathbf{q}, \tau')|^2 \bar{T}_{\tau', \tau''}^\mathbf{q} \bar{T}_{\tau', \tau''}^{\mathbf{k}-\mathbf{q}} + q^2 (k - q)^2 |A_+(\mathbf{q}, \tau')|^2 |A_+(\mathbf{k} - \mathbf{q}, \tau')|^2 T_{\tau', \tau''}^\mathbf{q} T_{\tau', \tau''}^{\mathbf{k}-\mathbf{q}} \right. \\ &\quad \left. + q(k - q) \left[\bar{T}_{\tau', \tau''}^\mathbf{q} \bar{T}_{\tau', \tau''}^{\mathbf{k}-\mathbf{q}} A_+(\mathbf{q}, \tau') A_+^{*\prime}(\mathbf{q}, \tau') A_+(\mathbf{k} - \mathbf{q}, \tau') A_+^{*\prime}(\mathbf{k} - \mathbf{q}, \tau') \right. \right. \\ &\quad \left. \left. + T_{\tau', \tau''}^\mathbf{q} T_{\tau', \tau''}^{\mathbf{k}-\mathbf{q}} A'_+(\mathbf{q}, \tau') A'_+^*(\mathbf{q}, \tau') A'_+(\mathbf{k} - \mathbf{q}, \tau') A'_+^*(\mathbf{k} - \mathbf{q}, \tau') \right] \right\}. \end{aligned} \quad (\text{B7})$$

The cross term between A and A' can be written as

$$\begin{aligned} A_+(\mathbf{q}, \tau'') A_+^{*\prime}(\mathbf{q}, \tau'') &= A_+^{(R)}(\mathbf{q}, \tau'') A_+^{(R)\prime}(\mathbf{q}, \tau'') + A_+^{(I)}(\mathbf{q}, \tau'') A_+^{(I)\prime}(\mathbf{q}, \tau'') \\ &\quad + i \left\{ A_+^{(I)}(\mathbf{q}, \tau'') A_+^{(R)\prime}(\mathbf{q}, \tau'') - A_+^{(R)}(\mathbf{q}, \tau'') A_+^{(I)\prime}(\mathbf{q}, \tau'') \right\} \\ &= \text{Re}[A_+(\mathbf{q}, \tau'') A_+^{*\prime}(\mathbf{q}, \tau'')] + i \text{Im}[A_+(\mathbf{q}, \tau'') A_+^{*\prime}(\mathbf{q}, \tau'')]. \end{aligned} \quad (\text{B8})$$

This imaginary contribution is obtained from the normalization of the wave function giving it a constant value $1/2$. With the proper renormalization one removes this vacuum contribution. The last line in Eq. (B7) becomes

$$\bar{T}_{\tau', \tau''}^\mathbf{q} \bar{T}_{\tau', \tau''}^{\mathbf{k}-\mathbf{q}} \text{Re}[A_+^\mathbf{q}(\tau') A_+^{*\prime\mathbf{q}}(\tau')] \text{Re}[A_+^{\mathbf{k}-\mathbf{q}}(\tau') A_+^{*\prime\mathbf{k}-\mathbf{q}}(\tau')] + T_{\tau', \tau''}^\mathbf{q} T_{\tau', \tau''}^{\mathbf{k}-\mathbf{q}} \text{Re}[A_+^\mathbf{q}(\tau') A_+^{*\prime\mathbf{q}}(\tau')] \text{Re}[A_+^{\mathbf{k}-\mathbf{q}}(\tau') A_+^{*\prime\mathbf{k}-\mathbf{q}}(\tau')]. \quad (\text{B9})$$

To simplify the integration on q we use

$$|\epsilon_{-\lambda}^i(\mathbf{p}_1) \epsilon_+^i(\mathbf{p}_2)|^2 = \frac{1}{4} \left(1 + \lambda \frac{\mathbf{p}_1 \cdot \mathbf{p}_2}{p_1 p_2} \right)^2, \quad (\text{B10})$$

and the second line of Eq. (B7) becomes

$$\int d^3\mathbf{q} \frac{1}{16} \left(1 + s \frac{\mathbf{k} \cdot \mathbf{q}}{kq} \right) \left(1 + s' \frac{\mathbf{k} \cdot \mathbf{q}}{kq} \right) \left(1 + s \frac{\mathbf{k} \cdot (\mathbf{k} - \mathbf{q})}{k|\mathbf{k} - \mathbf{q}|} \right) \left(1 + s' \frac{\mathbf{k} \cdot (\mathbf{k} - \mathbf{q})}{k|\mathbf{k} - \mathbf{q}|} \right). \quad (\text{B11})$$

As we are numerically solving the gauge mode equations of motion until the end of inflation, with an unknown analytical solution, we will try to use the semi-analytical approach explained in section II to obtain these correlation functions. Integrating until $\epsilon_H = 2$ for several modes we get the gauge mode amplitude and velocity spectrums where they are expected to be at a maximum, just before the onset of a radiation dominated universe. Using the transfer functions, T and \bar{T} we can relate both derivatives and gauge field amplitudes at a given time τ to its values at the end of inflation and to write

$$\begin{aligned} \langle h_s(\mathbf{k}) h_{s'}(\mathbf{k}') \rangle &= \frac{2}{(2\pi)^3} \frac{H^4}{m_P^4} \delta(\mathbf{k} + \mathbf{k}') \int d\tau' d\tau'' \tau'^2 \tau''^2 G_k(\tau, \tau') G_k(\tau, \tau'') \\ &\int d^3\mathbf{q} \frac{1}{16} \left(1 + s \frac{\mathbf{k} \cdot \mathbf{q}}{kq} \right) \left(1 + s' \frac{\mathbf{k} \cdot \mathbf{q}}{kq} \right) \left(1 + s \frac{\mathbf{k} \cdot (\mathbf{k} - \mathbf{q})}{k|\mathbf{k} - \mathbf{q}|} \right) \left(1 + s' \frac{\mathbf{k} \cdot (\mathbf{k} - \mathbf{q})}{k|\mathbf{k} - \mathbf{q}|} \right) \times \\ &\left\{ |A_+^{\tau_e}(\mathbf{q})|^2 |A_+^{\tau_e}(\mathbf{k} - \mathbf{q})|^2 \bar{T}_{\tau', \tau_e}^\mathbf{q} \bar{T}_{\tau', \tau_e}^{\mathbf{k}-\mathbf{q}} \bar{T}_{\tau'', \tau_e}^\mathbf{q} \bar{T}_{\tau'', \tau_e}^{\mathbf{k}-\mathbf{q}} + q^2 (k - q)^2 |A_+^{\tau_e}(\mathbf{q})|^2 |A_+^{\tau_e}(\mathbf{k} - \mathbf{q})|^2 T_{\tau', \tau_e}^\mathbf{q} T_{\tau', \tau_e}^{\mathbf{k}-\mathbf{q}} T_{\tau'', \tau_e}^\mathbf{q} T_{\tau'', \tau_e}^{\mathbf{k}-\mathbf{q}} \right. \\ &\quad \left. + q(k - q) \left(|A_+^{\tau_e}(\mathbf{q}) A_+^{*\tau_e}(\mathbf{q})| |A_+^{\tau_e}(\mathbf{k} - \mathbf{q}) A_+^{*\tau_e}(\mathbf{k} - \mathbf{q})| T_{\tau', \tau_e}^\mathbf{q} T_{\tau', \tau_e}^{\mathbf{k}-\mathbf{q}} \bar{T}_{\tau'', \tau_e}^\mathbf{q} \bar{T}_{\tau'', \tau_e}^{\mathbf{k}-\mathbf{q}} \right. \right. \\ &\quad \left. \left. + |A_+^{\tau_e}(\mathbf{q}) A_+^{*\tau_e}(\mathbf{q})| |A_+^{\tau_e}(\mathbf{k} - \mathbf{q}) A_+^{*\tau_e}(\mathbf{k} - \mathbf{q})| \bar{T}_{\tau', \tau_e}^\mathbf{q} \bar{T}_{\tau', \tau_e}^{\mathbf{k}-\mathbf{q}} T_{\tau'', \tau_e}^\mathbf{q} T_{\tau'', \tau_e}^{\mathbf{k}-\mathbf{q}} \right) \right\}. \end{aligned} \quad (\text{B12})$$

where to simplify the notation we have written $\text{Re}[A_+^{\tau_e}(\mathbf{q}) A_+^{*\tau_e}(\mathbf{q})] = |A_+^{\tau_e}(\mathbf{q}) A_+^{*\tau_e}(\mathbf{q})|$.

Using the results in Eqs. (37) and (38) with the functions (39), (40) and (41) for the amplitudes at the end of inflation we find the result in (42)

$$\begin{aligned}
\langle h_s h_{s'} \rangle &= \frac{2}{(2\pi)^3} \frac{H^4}{m_P^4} \frac{(a_e H_e)^5}{k^8} \int_0^\infty \int_0^\infty dx_1 dx_2 (\sin x_1 - x_1 \cos x_1) (\sin x_2 - x_2 \cos x_2) \\
&\int_0^\infty d\tilde{q} \int_0^{2\pi} \frac{2\pi}{16} \tilde{q}^2 d\theta (1 + s \cos \theta) (1 + s' \cos \theta) \left(1 + s \frac{1 - \frac{\tilde{q} \cos \theta}{k}}{\sqrt{1 + \frac{\tilde{q}^2}{k^2} - 2 \frac{\tilde{q}}{k} \cos \theta}} \right) \left(1 + s' \frac{1 - \frac{\tilde{q} \cos \theta}{k}}{\sqrt{1 + \frac{\tilde{q}^2}{k^2} - 2 \frac{\tilde{q}}{k} \cos \theta}} \right) \\
&(\tilde{q}^2 (\tilde{k} - \tilde{q})^2 |A_{end}(\tilde{q})|^2 |A_{end}(\tilde{k} - \tilde{q})|^2 T_{\tilde{q}}^{x_1} T_{\tilde{q}}^{x_2} T_{\tilde{k}-\tilde{q}}^{x_1} T_{\tilde{k}-\tilde{q}}^{x_2} \\
&+ |A'_{end}(\tilde{q})|^2 |A'_{end}(\tilde{k} - \tilde{q})|^2 \bar{T}_{\tilde{q}}^{x_1} \bar{T}_{\tilde{q}}^{x_2} \bar{T}_{\tilde{k}-\tilde{q}}^{x_1} \bar{T}_{\tilde{k}-\tilde{q}}^{x_2} \\
&+ \tilde{q}(\tilde{k} - \tilde{q}) |AA'_{end}(\tilde{q})| |AA'_{end}(\tilde{k} - \tilde{q})| (T_{\tilde{q}}^{x_1} \bar{T}_{\tilde{q}}^{x_2} T_{\tilde{k}-\tilde{q}}^{x_1} \bar{T}_{\tilde{k}-\tilde{q}}^{x_2} + T_{\tilde{q}}^{x_2} \bar{T}_{\tilde{q}}^{x_1} T_{\tilde{k}-\tilde{q}}^{x_2} \bar{T}_{\tilde{k}-\tilde{q}}^{x_1})), \tag{B13}
\end{aligned}$$

where $x = -k\tau$ and $\tilde{q} = q/(a_e H_e)$.

Acknowledgments

This work has been partially supported by MICINN (PID2019-105943GB-I00/AEI/10.13039/501100011033) and ‘‘Junta de Andaluc a’’ grants P18-FR-4314. ATM is supported by FCT grant SFRH/BD/144803/2019.

-
- [1] A. H. Guth, Phys. Rev. D **23**, 347 (1981).
 - [2] A. D. Linde, Phys. Lett. B **108**, 389 (1982).
 - [3] A. Albrecht and P. J. Steinhardt, Phys. Rev. Lett. **48**, 1220 (1982).
 - [4] B. D. Fields, P. Molaro, and S. Sarkar, Chin. Phys. C **38**, 339 (2014), 1412.1408.
 - [5] P. A. Zyla et al. (Particle Data Group), PTEP **2020**, 083C01 (2020).
 - [6] D. G. Figueroa and E. H. Tanin, JCAP **10**, 050 (2019), 1811.04093.
 - [7] E. Pajer and M. Peloso, Class. Quant. Grav. **30**, 214002 (2013), 1305.3557.
 - [8] V. Domcke, V. Guidetti, Y. Welling, and A. Westphal, JCAP **09**, 009 (2020), 2002.02952.
 - [9] E. V. Gorbar, K. Schmitz, O. O. Sobol, and S. I. Vilchinskii, Phys. Rev. D **104**, 123504 (2021), 2109.01651.
 - [10] A. Caravano, E. Komatsu, K. D. Lozanov, and J. Weller (2022), 2204.12874.
 - [11] M. M. Anber and L. Sorbo, JCAP **0610**, 018 (2006), astro-ph/0606534.
 - [12] L. Sorbo, JCAP **06**, 003 (2011), 1101.1525.
 - [13] M. M. Anber and L. Sorbo, Phys. Rev. **D85**, 123537 (2012), 1203.5849.
 - [14] J. Garc a-Bellido, M. Peloso, and C. Unal, JCAP **1612**, 031 (2016), 1610.03763.
 - [15] N. Bartolo et al., JCAP **12**, 026 (2016), 1610.06481.
 - [16] N. Barnaby and M. Peloso, Phys. Rev. Lett. **106**, 181301 (2011), 1011.1500.
 - [17] N. Barnaby, R. Namba, and M. Peloso, JCAP **1104**, 009 (2011), 1102.4333.
 - [18] A. Linde, S. Mooij, and E. Pajer, Phys. Rev. **D87**, 103506 (2013), 1212.1693.
 - [19] G. B. Field and S. M. Carroll, Phys. Rev. **D62**, 103008 (2000), astro-ph/9811206.
 - [20] P. Adshead, J. T. Giblin, T. R. Scully, and E. I. Sfakianakis, JCAP **1610**, 039 (2016), 1606.08474.
 - [21] M. M. Anber and L. Sorbo, Phys. Rev. **D81**, 043534 (2010), 0908.4089.
 - [22] K. V. Berghaus, P. W. Graham, and D. E. Kaplan, JCAP **03**, 034 (2020), 1910.07525.
 - [23] M. Laine and S. Procacci, JCAP **06**, 031 (2021), 2102.09913.
 - [24] A. E. Nelson and J. Scholtz, Phys. Rev. **D84**, 103501 (2011), 1105.2812.
 - [25] P. Arias, D. Cadamuro, M. Goodsell, J. Jaeckel, J. Redondo, and A. Ringwald, JCAP **1206**, 013 (2012), 1201.5902.
 - [26] P. W. Graham, J. Mardon, and S. Rajendran, Phys. Rev. **D93**, 103520 (2016), 1504.02102.
 - [27] P. Agrawal, N. Kitajima, M. Reece, T. Sekiguchi, and F. Takahashi, Phys. Lett. **B801**, 135136 (2020), 1810.07188.
 - [28] K. Nakayama, JCAP **08**, 033 (2020), 2004.10036.
 - [29] Y. Nakai, R. Namba, and Z. Wang, JHEP **12**, 170 (2020), 2004.10743.
 - [30] B. Salehian, M. A. Gorji, H. Firouzjahi, and S. Mukohyama (2020), 2010.04491.
 - [31] H. Firouzjahi, M. A. Gorji, S. Mukohyama, and B. Salehian (2020), 2011.06324.
 - [32] M. Bastero-Gil, J. Santiago, L. Ubaldi, and R. Vega-Morales, JCAP **1904**, 015 (2019), 1810.07208.
 - [33] M. Bastero-Gil, J. Santiago, R. Vega-Morales, and L. Ubaldi, JCAP **02**, 015 (2022), 2103.12145.
 - [34] V. Domcke and K. Mukaida (2018), 1806.08769.
 - [35] V. Domcke, Y. Ema, and K. Mukaida, JHEP **02**, 055 (2020), 1910.01205.

- [36] M. Giovannini and M. E. Shaposhnikov, Phys. Rev. D **57**, 2186 (1998), hep-ph/9710234.
- [37] M. M. Anber and E. Sabancilar, Phys. Rev. D **92**, 101501 (2015), 1507.00744.
- [38] T. Fujita and K. Kamada, Phys. Rev. D **93**, 083520 (2016), 1602.02109.
- [39] Y. Cado and E. Sabancilar, JCAP **04**, 047 (2017), 1611.02293.
- [40] D. Jiménez, K. Kamada, K. Schmitz, and X.-J. Xu, JCAP **12**, 011 (2017), 1707.07943.
- [41] V. Domcke, B. von Harling, E. Morgante, and K. Mukaida, JCAP **10**, 032 (2019), 1905.13318.
- [42] R. T. Co, A. Pierce, Z. Zhang, and Y. Zhao, Phys. Rev. **D99**, 075002 (2019), 1810.07196.
- [43] Y. Shtanov, J. H. Traschen, and R. H. Brandenberger, Phys. Rev. D **51**, 5438 (1995), hep-ph/9407247.
- [44] L. Kofman, A. D. Linde, and A. A. Starobinsky, Phys. Rev. D **56**, 3258 (1997), hep-ph/9704452.
- [45] O. O. Sobol, A. V. Lysenko, E. V. Gorbar, and S. I. Vilchinskii, Phys. Rev. D **102**, 123512 (2020), 2010.13587.
- [46] Y. Akrami et al. (Planck), Astron. Astrophys. **641**, A10 (2020), 1807.06211.
- [47] R. Kallosh, A. Linde, and D. Roest, JHEP **11**, 198 (2013), 1311.0472.
- [48] M. M. Anber and L. Sorbo, Phys. Rev. D **81**, 043534 (2010), 0908.4089.
- [49] M. C. Guzzetti, N. Bartolo, M. Liguori, and S. Matarrese, Riv. Nuovo Cim. **39**, 399 (2016), 1605.01615.
- [50] C. Caprini and D. G. Figueroa, Class. Quant. Grav. **35**, 163001 (2018), 1801.04268.
- [51] K. Yagi and N. Seto, Phys. Rev. D **83**, 044011 (2011), [Erratum: Phys.Rev.D 95, 109901 (2017)], 1101.3940.
- [52] L. E. Parker and D. Toms, *Quantum Field Theory in Curved Spacetime: Quantized Field and Gravity*, Cambridge Monographs on Mathematical Physics (Cambridge University Press, 2009), ISBN 978-0-521-87787-9, 978-0-521-87787-9, 978-0-511-60155-2.
- [53] N. Aggarwal et al., Living Rev. Rel. **24**, 4 (2021), 2011.12414.
- [54] N. Aggarwal, G. P. Winstone, M. Teo, M. Baryakhtar, S. L. Larson, V. Kalogera, and A. A. Geraci, Phys. Rev. Lett. **128**, 111101 (2022), 2010.13157.
- [55] N. Herman, A. Füzfa, L. Lehoucq, and S. Clesse, Phys. Rev. D **104**, 023524 (2021), 2012.12189.
- [56] F. Takahashi, W. Yin, and A. H. Guth, Phys. Rev. D **98**, 015042 (2018), 1805.08763.